

Optimal Fixture Design For Drilling in Elastically Deforming Plates

Khaled Wardak, Uri Tasch, Panos Charalambides
Department of Mechanical Engineering
University of Maryland, Baltimore County

Abstract

Software tools for computer-aided design (CAD) and finite element analysis (FEA) have been under continuous development in recent years. These methods can be applied to manufacturing in the area of advanced fixture design. Fixtures are an essential component of manufacturing and production. They are used to accurately position a component or workpiece in or within a machine-tool coordinate system, or with respect to another component. In material removal, the functionality of the fixture is to ensure that the workpiece is constrained such that the design requirements are met. The fixture performs this function by providing accurate and repeatable location of the datum surfaces of the part with respect to the axes of the machine tool, and by resisting motions, deflections and distortions of the workpiece under the influence of the cutting forces. It has been stated in the literature that approximately 40% of part rejects are attributed to poor fixture design. In material removal processes, major deviations of part dimensions beyond the design specifications are attributed to workpiece distortions and deformations that are due to the cutting forces and clamping intensities. Therefore, the focus of this research is to develop scientific methods that analyze and optimize fixture designs that minimize the errors of part dimensions. This would contribute to and further enhance the technology of the computer aided fixture design. This paper addresses the development of automated software tools that describe the shape and dimensions of 3D machined surfaces. The schemes utilize finite element methods (FEM) to automatically generate meshes of nontrivial geometric surfaces. Super elements and isoparametric mapping techniques are utilized. Automatic generation of FEM 3D meshes have been reported, yet these applications were limited to the use of tetrahedral elements with poor accuracy. The current paper utilizes twenty noded brick elements that accurately predicts workpiece deflections, and therefore when used to describe 3D machined surfaces, it will capture the resulting shape and dimensions of the workpiece with more accuracy. The current paper addresses the drilling operation and utilizes automatic FEM mesh generators coupled with inverse mapping techniques to predict the size and shape of the machined surface. Here, the workpiece is constrained in a fixture as it undergoes material removal due to the insertion of the drill bit. The deformations and dis-

tortions of the workpiece are modeled at discrete intervals throughout the drilling process. Such a model can be used for examining the effects of various fixture designs, as entailed to the accuracy and shape of the resulting drilled surfaces. This study will lead to the generation of optimal fixture designs. The latter will be the result of using the current mesh generation techniques coupled with optimization algorithms that minimize selected objective functions.

1 Introduction

This paper focuses on fixture layout design for machining applications, with emphasis placed on the drilling. When one machines a workpiece, it is essential to appropriately locate and constrain the part. Machining fixtures are designed to constrain a deformable workpiece that is exposed to significant machining loads. The fixture ensures that the dimensions and shape of the machined part are within the required tolerances. Nixon[1] has reported that approximately 40% of part rejects are due to dimensioning errors that are attributed to poor fixturing design.

Researchers who have addressed fixturing design introduced Automated Computer Aided Fixture Design that is based on CAD model of the part[2]. This design scheme has not yet been fully implemented on the factory floor. Fixture design algorithms that use rigid body models for the workpiece are reported in [2-5]. Here, rigid body kinematics under various geometrical constraints are used for designing fixtures that prevent workpiece motions. However, this approach fails to account for the elastic deformations of the workpiece, as it is exposed to significant machining loads.

In addition to the rigid body kinematics approach, more recent studies[3,4,6] have addressed fixture optimization via the minimization of an objective function mainly based on the reaction forces at the locators and supports. The objective of these studies was to select the clamping locations associated with statically admissible minimal reaction forces. In those studies, it was hypothesized that minimizing the maximum normal reaction force led to fixturing designs which also minimize the workpiece deformations in the neighborhood of regions undergoing machining. In other studies, the elasticity of the workpiece was incorporated into fixture optimizing algorithms[7-9]

which were used in the cases of simple systems to evaluate the validity of the min-max normal reaction force. Their finding, suggest that in most instances, the elasticity of the workpiece may substantially alter the optimal fixture conditions which can not always be predicted using the min-max normal reaction approach.

The application of FEM and optimization techniques have been reported by researchers who minimized workpiece deformations. Lee and Haynes [7] first employed the FEM technique to compute the objective function which was defined as the maximum work done by the clamping and machining forces. Here, the deformation index was the maximum stress applied on the workpiece. Such studies emphasize the consequence and importance of part deformation and stress with respect to the necessary number of fixturing elements; however, the methodologies utilized do not contain a systematic method to optimize the fixture configuration. In the optimum design of fixture layout outlined by Menassa and Devries [8], the optimization scheme was subdivided into two modules: FEM and optimization. In these studies, the objective function was selected as the displacement of surface nodes of the unmachined workpiece. Po [9] utilized the ANSYS software coupled with optimization algorithms to further enhance the methodology initiated by Menassa and Devries by taking into account the elastic behavior of the fixturing components. The objective function used by Po also consisted of the displacements of selected surface nodes.

In reality, workpieces are deformable, and therefore the magnitude and directions of the deformations are a result of the fixture configuration and the action of the cutting and clamping forces. These deformations clearly affect the dimensions of the machined workpiece and result in part dimensions that deviate from their nominal values and possibly exceed the allowable tolerances.

Moreover, as precision requirements for parts produced are increased, the effects of workpiece deformations on the machined dimensions are no longer negligible. Fixtures designed in traditional ways may no longer have the capability of producing high precision parts. The considerations of workpiece deformations and the development of mathematical models that predict the dimensions of the machined surfaces become necessary for fixture layout design for precision machining.

The most realistic and logical approach to minimizing the effects of workpiece deformations on workpiece dimensions is to develop mathematical models which have the capability of predicting the geometry of machined surfaces upon completion of the machining process. The goal of this paper is to devise such mathematical tools, that capture the shape and ge-

ometry of the machined surfaces generated through drilling operations. These tools will be based on the finite element(FE) model, and will entail schemes that handle material removal strategies.

2 Research Methodology

This paper provides a methodology for describing the shape and dimensions of machined surfaces following machining and incorporates the effects of removed material on the workpiece deformation state and the dimensions of machined regions. The essence of the methodology is to predict the location of the series of points that come in contact with the drill bit outer surface as the drill penetrates through the deformed workpiece. These points are in a deformed state and have traveled during machining from their original location. The identification of the original location of these points will provide the shape and the dimensions of the hole subsequent to machining. In the deformed state, these points form a perfect cylinder while coming into contact with the drill bit as the drill bit penetrates the workpiece. It is assumed that the drill bit is rigid. This approach can be further illustrated by a two dimensional eight noded isoparametric element shown in Figure 2. Assuming that the nodes are displaced from their original locations after the element deforms from coordinates x_i, y_i to x'_i, y'_i . There exists a line containing points p' and q' on the drill bit outer surface, and these points are displaced from positions p and q. Assuming that the curve containing p and q becomes a straight line containing p' and q', one needs to determine p and q from the knowledge of the coordinates of p' and q'. The coordinates of p' and q' are known quantities with respect to a global reference frame.

Utilizing the finite element method, one can write:

$$x = \sum_{i=1}^8 N_i x_i \quad (1)$$

$$y = \sum_{i=1}^8 N_i y_i$$

$$\bar{u} = u\bar{i} + v\bar{j} \quad (2)$$

$$u = \sum_{i=1}^8 N_i u_i \quad (3)$$

$$v = \sum_{i=1}^8 N_i v_i$$

$$x' = x + u = \sum_{i=1}^8 N_i x'_i \quad (4)$$

$$y' = y + v = \sum_{i=1}^8 N_i y'_i$$

N_i are the shape functions which consist of variables ξ and η ; u and v are displacements; i refers to nodal quantities, primed values are for post-deformation. From equation 4, it is apparent that x' and y' are known quantities in addition to x'_i and y'_i which are the locations of the displaced nodes. This results in two coupled nonlinear equations which may be solved for ξ and η . Subsequently, ξ and η may be substituted in equation 1 to determine x and y corresponding to the undeformed location. The same approach is used in this paper, however dealing with a three dimensional case using twenty noded brick elements. In this case, one is dealing with three coupled nonlinear equations which are solved using Newton's method embedded in a globally convergent strategy. The methodology is applied to a rectangular plate of arbitrary dimensions undergoing a drilling process with a hole of arbitrary diameter and position (Figure 1). The finite element method is applied with a pre-designed automatic mesh generator to incorporate the strategy. The hole is drilled and material is removed in accordance with the workpiece deformation state as the drill bit is inserted. As the machining process is completed, the workpiece returns to its initial undeformed state, thereby the system is assumed to be linear and elastic. The cylindrical mesh region where the hole is located, assumes the shape and dimensions of the hole subsequent to machining. At discrete points, error estimates are taken between the nominal hole and the machined hole. In the current paper, it is assumed that the most significant effect of the removed material on the deformation state near the machining region occurs when the drilling process is almost completed. Therefore, for computational efficiency purposes, the workpiece geometry is discretized finite elements near the end of the machining process. Here, volumes that come in contact with the drill outer surface are removed as stated above.

3 Three Dimensional Finite Element Modeling

The finite element method involves the approach of obtaining numerical approximations to the exact solutions of partial differential equations. In the case of solid mechanics, the finite element method is used to calculate approximate solutions to the boundary value problems of elasticity. The finite element method always consists of an algorithm which involves three steps[10]:

1. Pre-Processing: Describing the geometry, material properties selection, state the boundary

conditions of the domain. Discretize the domain through meshing. This consists of creating nodes and finite elements within the domain.

2. Processing: Solve the finite element equations resulting from the boundary value problem for all of the pertinent field quantities: displacements, strains, stresses, temperatures, plasticity, etc.
3. Post-Processing: Display the results in a meaningful way, and verify the correctness of the results.

4 Automatic Mesh Generation Procedures

In this study, we present an integrated approach to 3-D FEM modeling which encompasses the above three steps and allows for process optimization as part of post-processing. In the section below, we shall present in brief, the pre-processing mesh generation method developed for this study. An automatic mesh generator was developed using 20 noded brick elements. The essence of the present scheme is the use of 'isoparametric' curvilinear mapping of hexahedrals which allow a coordinate mapping of curvi-linear and Cartesian coordinates. In this case, we can write[11]:

$$\begin{aligned} x &= \sum_{i=1}^{20} N_i x_i \\ y &= \sum_{i=1}^{20} N_i y_i \\ z &= \sum_{i=1}^{20} N_i z_i \end{aligned} \quad (5)$$

in which N_i is the shape function associated with each node and defined in terms of standard element coordinate system ξ, η, ζ which has values ranging from -1 to 1 on opposite sides (Figure 3).

$$\begin{aligned} N_i &= \frac{1}{8}(1 + \xi\xi_i)(1 + \eta\eta_i)(1 + \zeta\zeta_i)(\xi\xi_i + \eta\eta_i + \zeta\zeta_i - 2) \\ i &= 1, 2, \dots, 8 \\ N_i &= \frac{1}{4}(1 - \xi^2)(1 + \eta\eta_i)(1 + \zeta\zeta_i) \quad i = 9, 11, 17, 19 \\ N_i &= \frac{1}{4}(1 - \eta^2)(1 + \xi\xi_i)(1 + \zeta\zeta_i) \quad i = 10, 12, 18, 20 \\ N_i &= \frac{1}{4}(1 - \zeta^2)(1 + \xi\xi_i)(1 + \eta\eta_i) \quad i = 13, 14, 15, 16 \end{aligned} \quad (6)$$

If the Cartesian coordinate of the nodal points are known, then the Cartesian coordinate of any point in

the ξ , η , ζ space can be found using the above shape functions and mapping equation given in 6. If the entire region in which the mesh is to be generated could be described adequately by a hexahedral of the shape shown in Figure 4, then a mesh of any refinement can be automatically generated in the interior by specifying:

1. Cartesian coordinates of the 20 nodal points.
2. The number of subdivisions in ξ , η , ζ directions.

The above element is referred to as a super element. In addition, the hexahedral may be collapsed into a pentahedral by assigning the same Cartesian coordinate to adjacent nodes. Thus, the hexahedral is collapsed into a pentahedral super element, and a mesh of any refinement in the interior can be generated in the interior in a similar fashion.

The rectangular plate in Figure 1 is subdivided into eight sections, each section consisting of a pentahedral super element connected to a hexahedral super element. Transversing 360 degrees, the eight connected pentahedrals form a cylindrical region at an arbitrary location, and the hexahedrals span the remaining regions of the rectangular plate. An arbitrary number of elements can be generated in the interior of the pentahedrals as well as the hexahedrals (Figure 5). The hexahedral mesh diverges as it moves away from the hole with an arbitrary value set by the user. Across the workpiece thickness, an arbitrary number of super elements can be selected (Figure 6), and in addition the user may select an arbitrary number of layers within each super element layer (Figure 7). Typical meshes generated using this approach are shown in Figure 5-Figure 8. Moreover, the user is capable of generating meshes containing pre-existing holes as shown in Figure 8.

5 Drilling Simulations

5.1 Statement of the Problem

A rectangular plate with $l_x=1.5$ inches, $L_x=3$ inches, $l_y=2$ inches, $L_y=4$ inches and $h=0.25$ inches is drilled using a drill bit of 0.75 inches diameter. Three supports are placed at the bottom surface (Figure 1). This manuscript uses the value of the drill thrust reported by Po[9], and similarly to the work performed by Menassa and Devries[8] and a case study reported by Po, the drill torque was neglected.

The problem under consideration is solved using the in-house DENDRO software[10] which allows for the implementation of the three basic finite element steps highlighted above.

5.2 Pre-processing

5.2.1 Geometry and mesh generation

The geometry of the plate (Figure 1) subject to the given boundary conditions as shown in Figure 9 was discretized using the previously discussed automatic mesh generator into 2,016 twenty noded brick elements and 9,795 nodes. Ten layers of super elements were generated across the thickness. Nine of the said layers were removed from the interior of the hole.

5.2.2 Material properties

The material of the finite element model was specified as homogeneous isotropic Aluminum having a Young's Modulus of $E=1.0e7$ psi, and Poisson's ratio of $\nu = .30$. Thus the above material properties were given as input variables to DENDRO via the "Material Property" pull-down menu option, during the pre-processing.

5.2.3 Boundary conditions

The boundary conditions were applied by using the menu labeled "boundary conditions", which contains choices of applying displacement and loading boundary conditions. Two types of boundary conditions are applied (see Figure 9).

- (a) Displacement boundary conditions which are imposed on parts of the body (usually surfaces or edges) on which the displacements are known. This boundary is also known as the displacement boundary of the body and is often denoted as S_u . For the model under consideration the displacement constraints imposed by the supports were modeled as frictionless roller supports, thereby negating displacement in the z direction (see Figure 9). We define the displacement boundary and displacement boundary conditions with respect to the global coordinate system shown in the above mentioned figures as follows with $z=0.0$:

$$S_u = \left\{ \begin{array}{l} x = 0.96060725, \quad y = 1.16749523 \\ x = -1.12785295, \quad y = 1.16741625 \\ x = 0.0, \quad y = -1.16608072 \end{array} \right. \quad (7)$$

on S_u $w = 0.0$.

- (b) Traction boundary conditions. These conditions are imposed on the surfaces subjected to external mechanical loads. These surfaces and/or collection of surfaces points are often denoted as S_T . In this case S_T and the related traction conditions are:

$$S_T = S - S_u \quad (8)$$

where S denotes the entire boundary of the body and S_u denotes the displacement boundary defined earlier in this section. $F_x = F_y = 0$ everywhere except on S_T . In this case, the drill thrust was applied such that:

$$\begin{aligned} x &= 0.0, \quad y = 0.0, \quad z = 0.025 \\ F_z &= -674lb \end{aligned} \quad (9)$$

The above displacement and traction boundary conditions were introduced during pre-processing using the appropriate DENDRO menu options. The resulting finite element model for is shown in Figure 9.

5.3 Processing

The governing equations of the finite element method can be obtained by minimizing the total potential energy of the system. Equation 10 is the resulting system of linear equations.

$$[K]\{u_N\} = \{F_N\} \quad \text{Governing FE Equation} \quad (10)$$

where $[K]$ is the global stiffness matrix; u_N is the global nodal displacement vector, and F_N represents the global nodal forces. The finite element model developed in section was solved using DENDRO version 4.1 using the "frontal method" option.

5.4 Post-processing

5.4.1 Displacement field and deformed mesh

Figure 11 shows the deformed configuration of the finite element mesh for the plate. This result was obtained using DENDRO post-processing menu options. The displaced configuration shown in Figure 11 was obtained using a displacement magnification factor equal to 10.0. Clearly, the linear, small deformations small strain model, produces deformations which are very small compared to the plate dimensions and as such a magnification factor is required to visually display the deformed configuration. The magnitude of the maximum deformation was a significant 0.1493 inches.

6 Discussion and Future Work

The current manuscript presents a mathematical model for describing the shape and dimensions of a hole subsequent to a drilling process. Thereby, the model is capable of predicting the error between nominal dimensions and the actual dimensions of the machined regions (Figure 12) by taking into account the elastic behavior of the workpiece as affected by the fixture component locations and the given machining loadings. The results show that the hole is enlarged beyond a height of 0.1 inches from the bottom surface, and it is reduced below a height of 0.1 inches (Figure 13). In Figure 13, frames 1-6 describe cross-sections of the hole examined at depths ranging from 0.0 to 0.25 inches and clearly show that dimensional errors between nominal and actual dimensions. This is as a result of the cylindrical region collapsing inward and outward from the center point as the drilling loads are applied. Figure 15 demonstrates the variation of support location on the fixture performance. Here, the sum of the norm of the errors between the nominal radius and the machined region is taken about 16 points in the x,y plane and 11 planes across the height h of the hole. The x coordinate of a single support is varied, and Figure 15 demonstrates that the curve has a minimum value, which suggests an optimal set of support locations can be identified.

It becomes clear that for optimization purposes the capability of the above mathematical models becomes instrumental in developing objective functions which minimize the error between actual machined and nominal dimensions. Therefore, in lieu of minimizing displacements of selected surface nodes which do not have the capability of predicting or minimizing machining errors, the said model provides the ability to explicitly describe the machined surface dimensions, and subsequently is capable of developing objective functions which after a minimization can optimize the fixture configuration automatically when incorporated with computer aided fixture design modules. For future work, the above mathematical models will take into account contact friction and the elasticity of the fixture components, and when coupled with optimization tools, the results will be a further enhancement in automated computer aided fixture design technologies.

7 References

1. Nixon F., Managing to achieve quality and reliability, McGraw Hill, Maidenhead, 1971.
2. Shirinzadeh, B., "Issues in the design of the reconfigurable fixture modules for robotic assembly," Journal of Manufacturing Systems, vol. 12, No.1, 1993.

3. Brost R. and Goldberg K. "A complete algorithm for synthesizing modular fixtures for polygonal parts," Proc. IEEE Robotics and Automation, San Diego, CA, 1994, pp. 535-542.
4. Liu J. and Strong D., "Sorrey of fixture design automation," Vol. 17 No.4A, 1993.
5. Varma V., Tasch U., "A New Representation for Robot Grasping Quality Measures," Robotica, vol. 13, pp. 287-295, 1995.
6. Herskovitz M. Tasch U., Teboulle M., "Towards A Mathematical Model of the Human Grasping Quality Sense," Journal of Robotic Systems, vol. 13, No. 13, pp. 25-34, 1996.
7. Lee, J.D. and Haynes, L.S., "Finite Element Analysis of Flexible Fixturing System," Transactions of the ASME, Journal of Engineering for Industry, Vol. 109, No.2, pp. 134-139, 1987.
8. Menassa, R.J. and Devries, W.R., "Optimization Methods Applied to Selecting Support Positions in Fixture Design," Transactions of the ASME, Journal of Engineering for Industry, Vol. 113, pp. 412, 1991.
9. Pong Chung-Gwo, "Optimum Fixture Layout Design" Ph.D. thesis, The Pennsylvania State University, August 1994.
10. Charalambides P. and Kuhn J., A Guide to Finite Element Modeling, The University of Maryland Baltimore County, 1996.
11. Zienkiewicz O.C. and Phillips D., "An Automatic Mesh Generation Scheme for Plane and Curved Surfaces by 'isoprametric' Co-ordinates," International Journal for Numerical Methods in Engineering, Vol. 3, pp. 519-528, 1971.

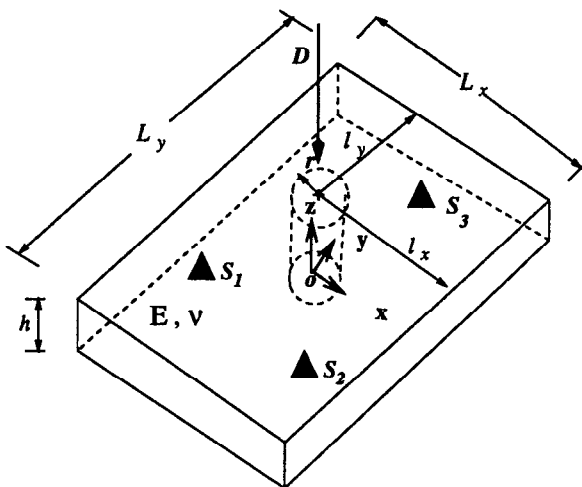


Figure 1: A Plate undergoing a drilling process.

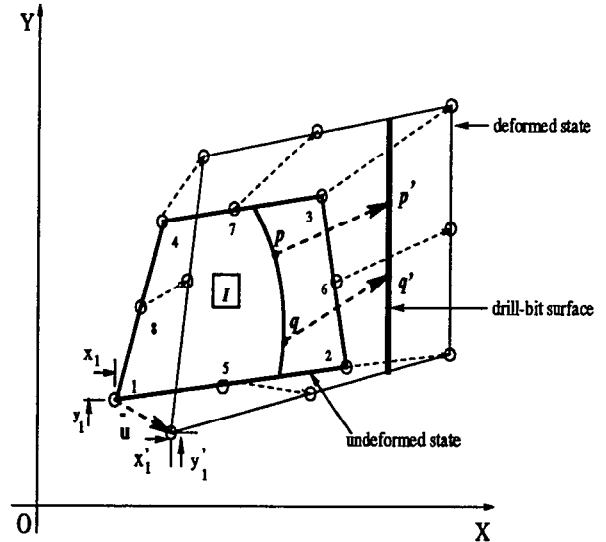


Figure 2: An eight noded isoparametric element.

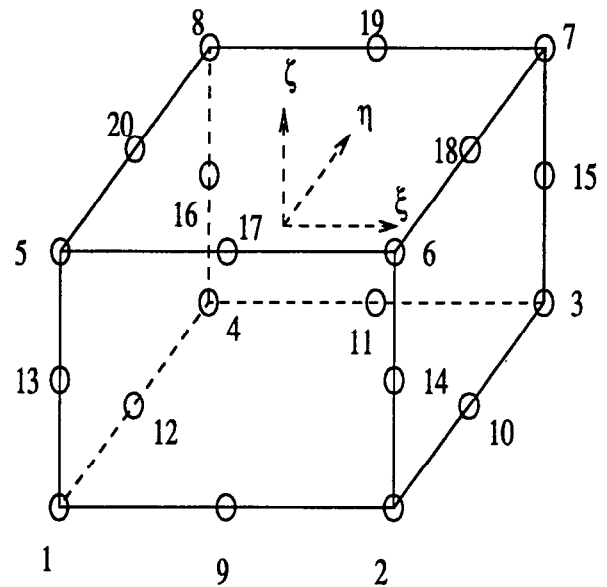


Figure 3: A standard element.

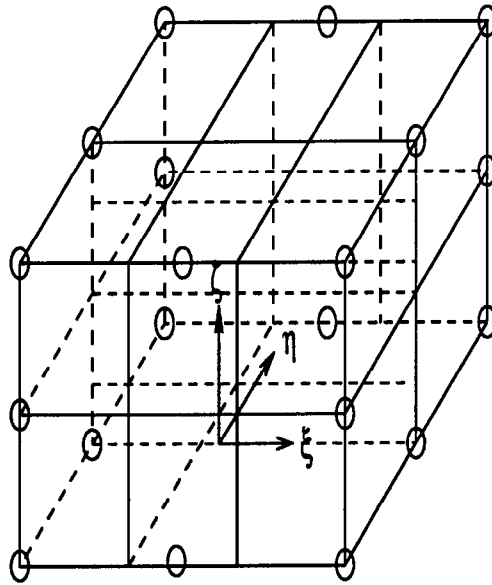


Figure 4: A super element.

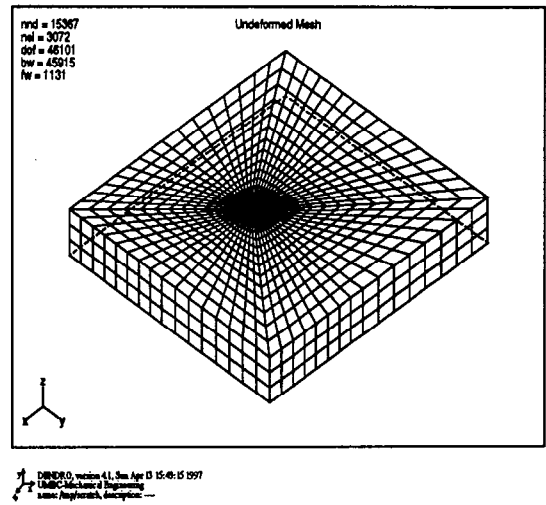


Figure 6: Mesh with n layers across the plate thickness.

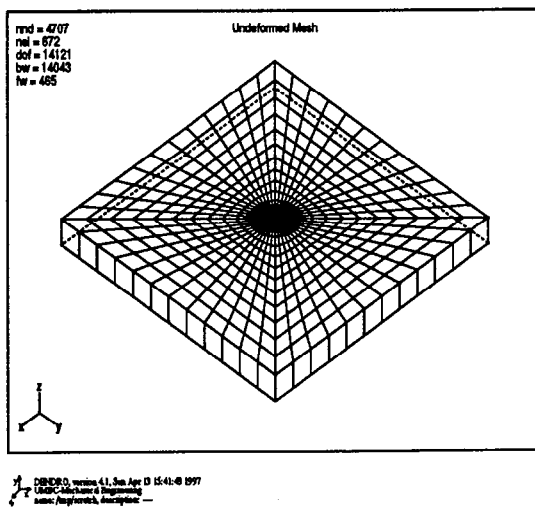


Figure 5: Automatic Mesh Generator Parameter Studies .

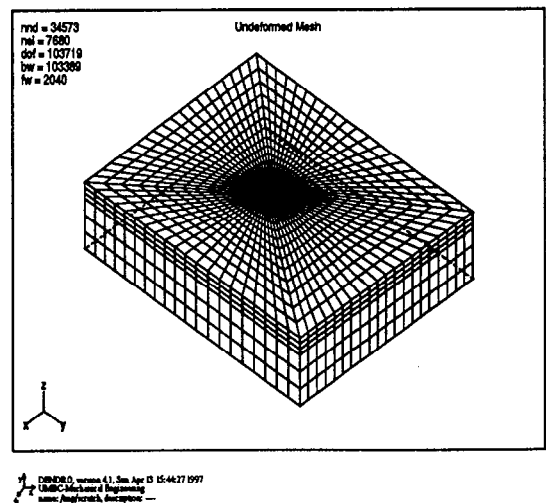
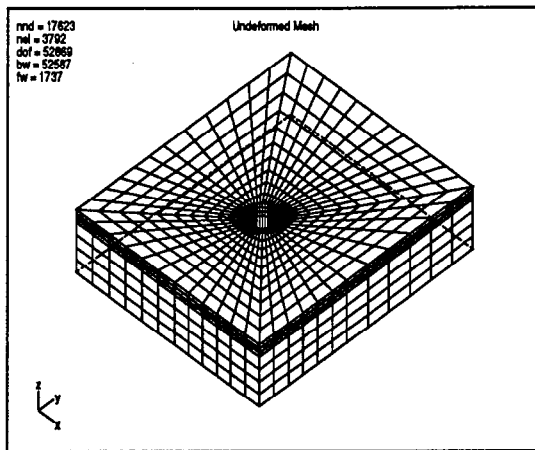


Figure 7: Modified super element layer across thickness .




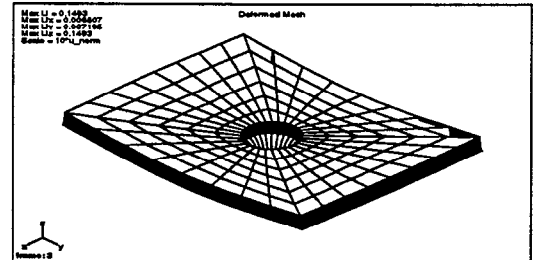
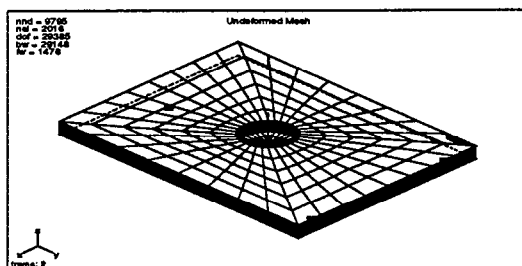

 DINERO, version 4.1, Sun Apr 13 15:45:34 1997
 UMBC-Mechanical Engineering
 name: AnyMesh, description: ---

Figure 8: Mesh with pre-existing hole.




 DINERO, version 4.0, Sun Apr 13 15:35:21 1997
 UMBC-Mechanical Engineering
 name: p16, description: ---

Figure 10: Deformed Plate under drilling load.




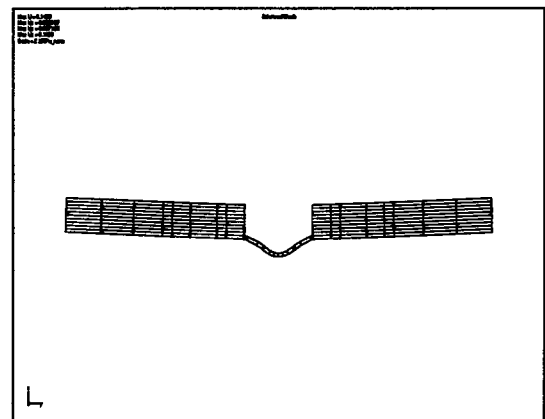

 DINERO, version 4.0, Sun Apr 13 15:34:13 1997
 UMBC-Mechanical Engineering
 name: p16, description: ---

Figure 9: Finite Element mesh with boundary conditions.




 DINERO, version 4.1, Thu Apr 10 14:57:08 1997
 UMBC-Mechanical Engineering
 name: AnyMesh, description: ---

Figure 11: Cross sectional view of Deformed Plate.

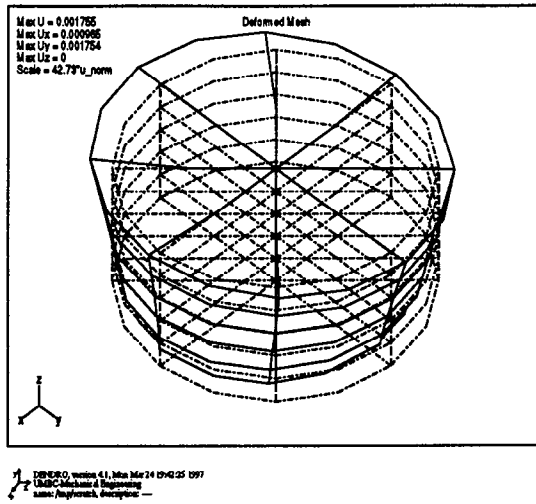


Figure 12: Nominal hole vs. machined hole.

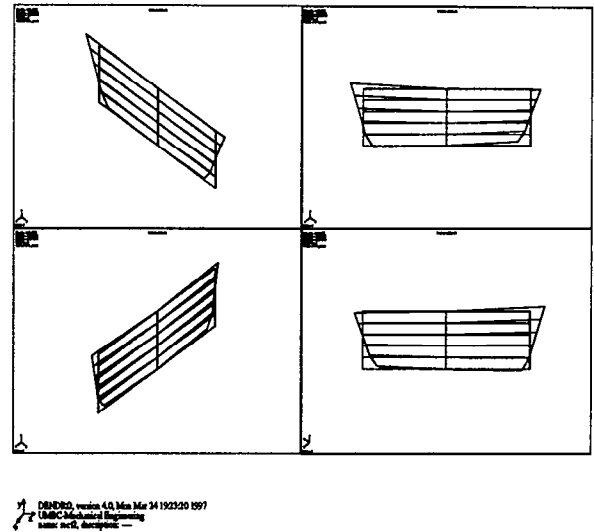


Figure 14: Cross sectional views of nominal vs machined hole, planes perpendicular to xy plane.

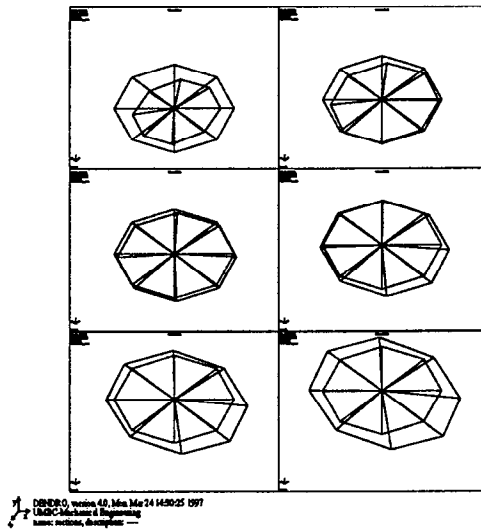


Figure 13: Error Estimates between Nominal and machined hole taken at depths ranging from 0-.25 inches.

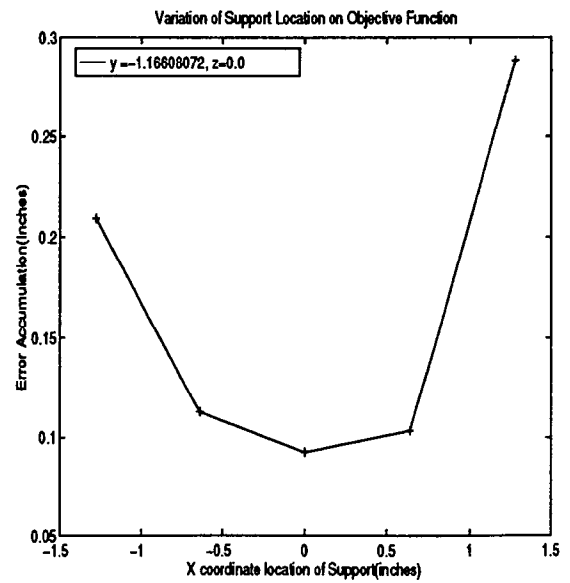


Figure 15: Error estimation.